Supporting Information

Efficient bifunctional catalysts for overall water splitting: Porous Fe-Mo oxide hybrids nanorods

Wei Chen[#a], Guangfu Qian[#a], Qinglian Xu[a], Chen Yu[a], Mengya Yu[a], Yijiang Xia*[b], Shibin Yin*[a]

[a] College of Chemistry and Chemical Engineering, Guangxi Key Laboratory of Petrochemical Resource Processing and Process Intensification Technology, School of Physical Science and Technology, State Key Laboratory of Processing for Non-Ferrous Metal and Featured Materials, Guangxi University, Nanning 530004, China.

[b] School of Mechanical and Ship Engineering, Beibu Gulf University, Qinzhou 535011, China

*Corresponding authors emails: xyj6678@foxmail.com (Y. Xia); yinshibin@gxu.edu.cn (S. Yin).

†These two authors contributed equally to this work.

1.1 Materials synthesis

Materials: Ni foam (NF), ferrous sulfate ($FeSO_4·7H_2O$), sodium dodecyl benzene sulfonate ($C_{18}H_{29}NaO_3S$), ammonium molybdate tetrahyfrate ($(NH_4)_6Mo_7O_{24}·2H_2O$), potassium hydroxide (KOH), and ethanol (C_2H_5OH) are purchased from Sinopharm Chemical Reagent Co., Ltd. The homemade deionized water (DI) used throughout all experiments is purified through a Millipore system. All the reagents and chemicals are used as received without further purification.

Preparation of $Fe_{1.966}O_{2.963}/Fe_2(MoO_4)_3$: Firstly, the NF is treated by ultrasonication in 1.0 M HCl solution to remove the possible surface oxide layer, after 30 min, it is cleaned with ethanol and deionized water for several times separately. $FeSO_4·7H_2O$ (0.75 mmol), $(NH_4)_6Mo_7O_{24}·2H_2O$ (0.75 mmol) and $C_{18}H_{29}NaO_3S$ (0.2 g) are dissolved in 30 mL deionized water. After gentle stirring for 5 min, the solution is transferred to a 50 mL Teflon-lined stainless-steel autoclave. The pretreated NF substrate (1 × 6 cm) is immersed into the solution. The autoclave is sealed and maintained at 120 °C for 48 h. After cooled down at room temperature, the obtained $Fe_{1.966}O_{2.963}/Fe_2(MoO_4)_3$ is taken out and washed with deionized water and ethanol, followed by drying at 60 °C for 12 h in a vacuum.

Preparation of Fe-Mo oxide hybrids: The prepared $Fe_{1.966}O_{2.963}/Fe_2(MoO_4)_3$ is used as substrate, it is put in a porcelain boat placed at the center of a tubular furnace. Subsequently, the furnace is purged with H_2/Ar atmosphere (5% H_2 and 95% Ar) for 15 min, then heated to 450 ^oC at a ramping rate of 5 ^oC min^{-1} and maintained for 2 h. After naturally cooled to room temperature, the Fe-Mo oxide hybrid is obtained.

Preparation of Pt/C and IrO_2/NF: The catalyst on a glassy carbon electrode (GCE) or NF is prepared as follows: The 20 wt% Pt/C or 40 wt% IrO_2/NF catalysts (5.0 mg) are dispersed in 1.0 mL solution containing 20.0 μL of 5 wt% Nafion solution and 0.98 mL of ethanol by ultrasonication for about 15 min. A 10.0 μL of the as-prepared ink is dropped on the surface of GCE or NF by using a micropipette, yielding a working electrode with catalysts loading of 0.05 mg cm^{-2} (Pt) or 0.1 mg cm^{-2} (IrO_2).

1.2 Catalysts characterization

X-ray photoelectron spectroscopy (XPS) is measured by a spectrometer ESCALab 250Xi (ThermoFisher Scientific, USA) with an Al X-ray source. The compositions of the as-prepared samples are characterized by X-ray diffraction (XRD) pattern on a SmartLab X-ray diffractometer (Rigaku Corp., Japan) using a copper K-edge X-rays (λ_{ka1} = 0.154056 nm). Scanning electron microscopy (SEM) measurements and energy dispersive spectrometer (EDS) analysis are performed by a FE-SEM SU8220 (Hitachi Corp., Japan) to characterize their morphologies and compositions. Scanning transmission electron microscopy (STEM) and energy dispersive X-ray spectroscopy (EDX) investigation are performed using a Titan ETEM G2 80-300 (FEI Co., USA) at an accelerating voltage of 200 kV, providing the information of particle size distribution and the composition of catalysts. The Brunauer-Emmett-Teller (BET) surface area and porous structures are tested by using an accelerated surface area and porosimetry analyzer (Micromeritics Instrument Corp, ASAP 2020 M + C, analysis adsorptive: N_2).

2. Additional figures and tables

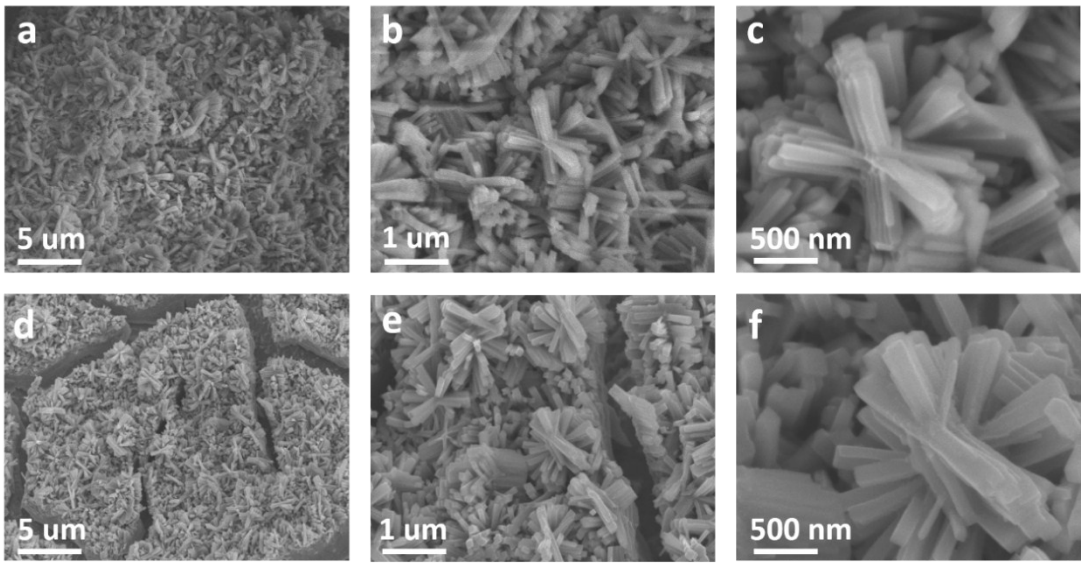

Fig. S1. The SEM images of $Fe_{1.966}O_{2.963}Fe_2(MoO_4)_3$ (a-c) and Fe-Mo oxide hybrids (d-f).

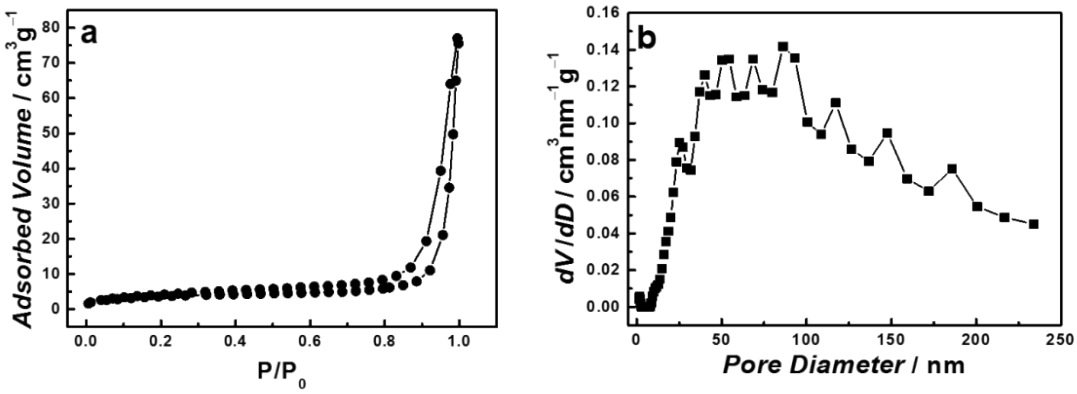

Fig. S2. Nitrogen adsorption-desorption isotherms (a) and pore size distribution curve (b) of Fe-Mo oxide hybrids.

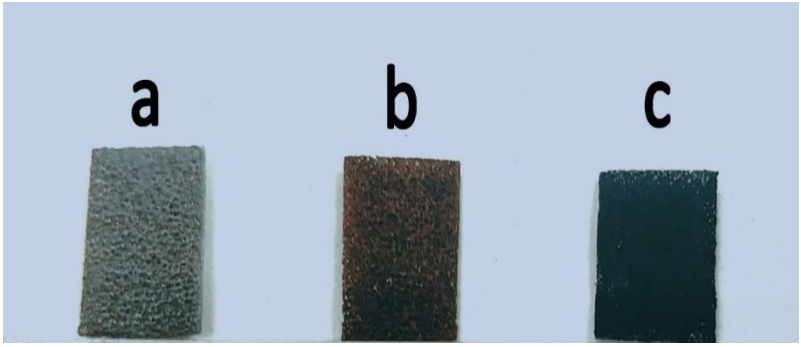

Fig. S3. Pictures of (a) NF, (b) $Fe_{1.966}O_{2.963}Fe_2(MoO_4)_3$, (c) Fe-Mo oxide hybrids.

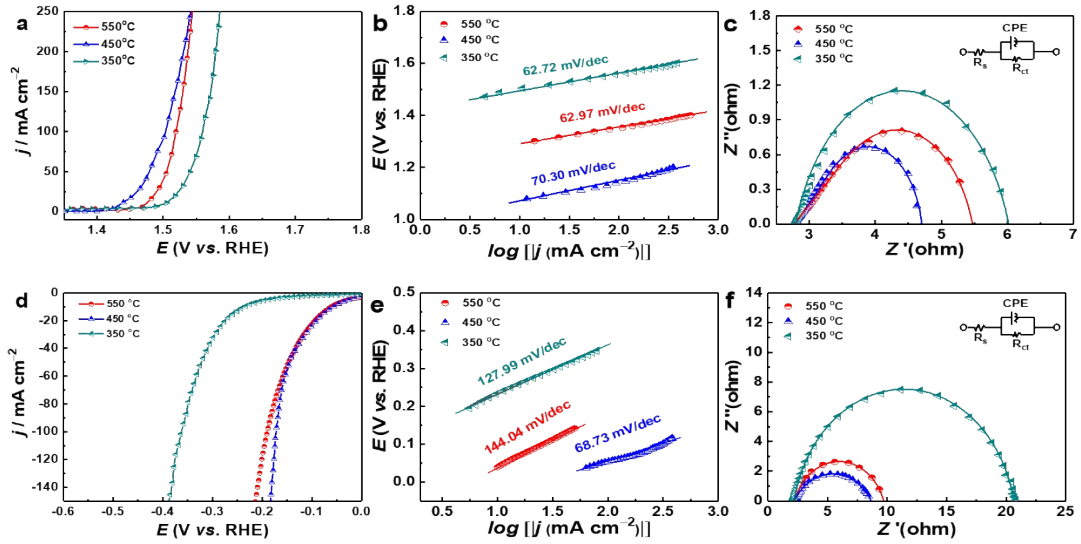

Fig. S4. (a) The OER polarization curves of the samples obtained at different calcination temperatures in 1.0 M KOH; (b) The corresponding Tafel plots and (c) Nyquist plots; (d) The HER polarization curves of different calcination temperatures in 1.0 M KOH; (e) The corresponding Tafel plots and (f) Nyquist plots.

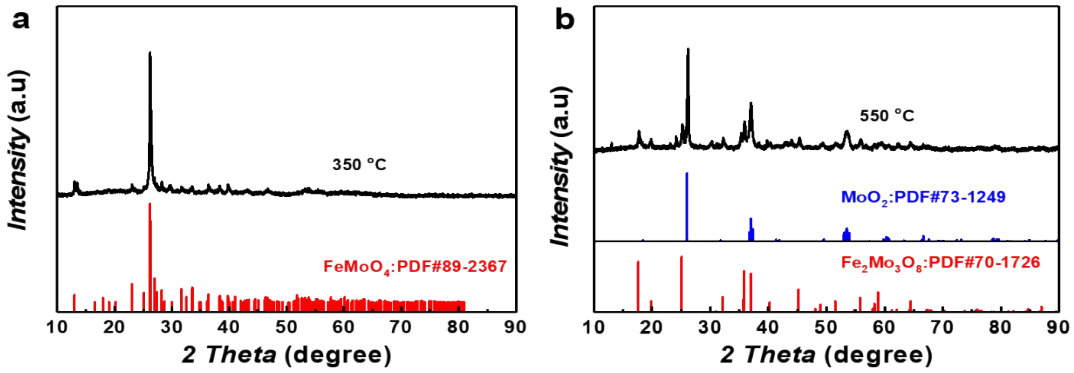

Fig. S5. XRD pattern of 350 °C (a) and 550 °C (b) calcination temperatures.

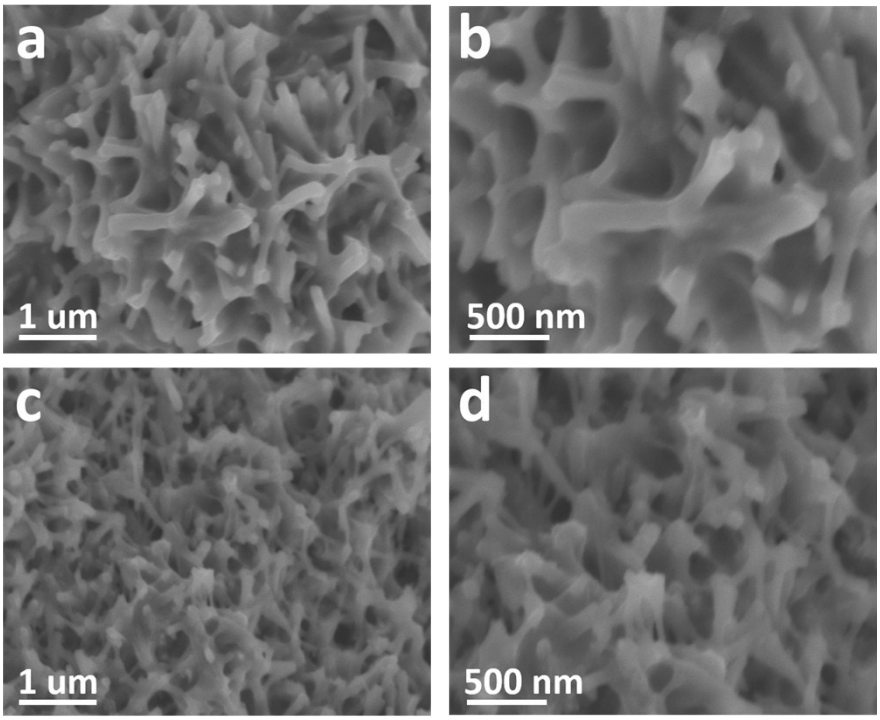

Fig. S6. The SEM images of Fe-Mo oxide hybrids after 85 h durability test in 1.0 M KOH for (a-b) OER and (c-d) HER at a constant current density (±200 mA cm^{-2}).

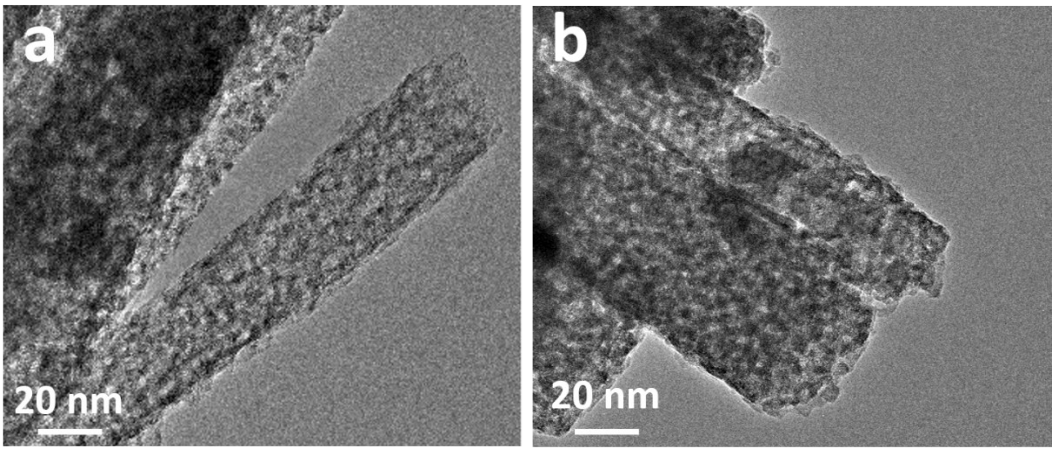

Fig. S7. The TEM images of Fe-Mo oxide hybrids after 85 h durability test in 1.0 M KOH for (a) OER and (b) HER at constant current densities (±200 mA cm^{-2}).

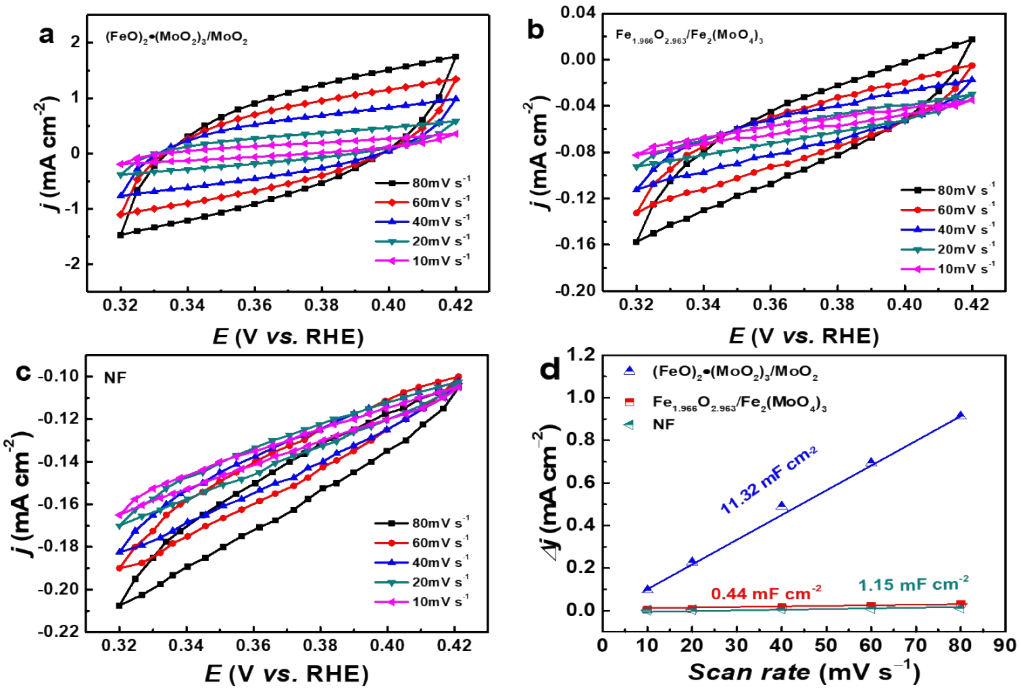

Fig. S8. (a-c) CVs for the samples in the non-faradaic capacitance current range at different scan rates; (d) The corresponding capacitive currents at 0.3718V *vs.* RHE as function of scan rates.

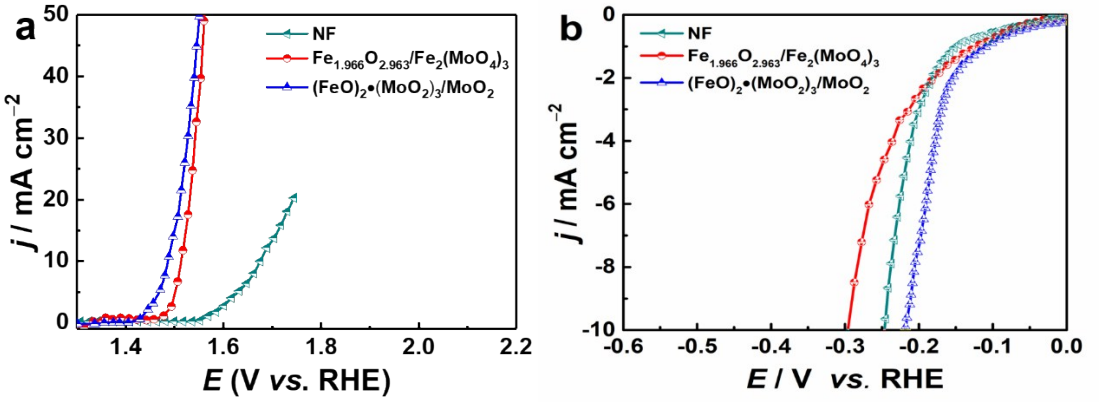

Fig. S9. (a) OER and (b) HER activities (current density) of the samples are normalized by their ECSA.

Table S1. Comparison OER and HER activities in 1.0 M KOH aqueous solution for Fe-Mo oxide hybrids with recently reported literatures.

Catalysts	Substrate	Overpotential at 10 mA cm^{-2} (mV)		Tafel slope (mV dec^{-1})		Ref.
		OER	HER	OER	HER	
Fe-Mo oxide hybrids nanorods	Ni foam	200	66	70.30	68.73	This work
(Ni, Fe)S_2@MoS_2	Carbon fiber paper	270	130	43.21	101.22	1
CoFe-LDH	Ni foam	250	58	35	46	2
$(NiCo)_2P$/NF	Ni foam	220	162	69	135	3
Porous Ni-Mo-S nanowire	Ni foam	—	79	—	103	4
Ni_2P-$NiSe_2$	carbon cloth	—	66	—	72.6	5
$CoFe_2O_4$/C	Ni foam	240	—	45	—	6
FeP@CNT	CNT	250	—	53	—	7
Ni_2Fe_1–Mo	GC	231	147	39	128	8
Ni_3N-NiMoN	carbon cloth	277	31	118	64	9
Carbide-anchored N-doped graphene/CNT hybrid	CNT	328	162	74	104.8	10
NiS_2/MoS_2	GC	—	204	—	65	11
Ni_2P/MoO_2@MoS_2	titanium foil	280	159	85	77	12
CoS_2 –TiO_2	GC	231	198	92	61	13
Fe–Mn–O hybrid	carbon cloth	273	—	63.9	—	14
Co@N-CNTs@rGO	graphene oxide	—	108	—	55	15
O-CoMoS	carbon fiber cloth	272	97	45	70	16
MoP NWAs/CFP	Carbon fiber paper	—	52	—	40	17
MoS_2/FNS/FeNi	FeNi foam	204	120	28.1	45	18
MM'-NHCNPs	GC	350	—	58	—	19
NP-$NiFe_2O_4$/SWNTs	CNT	247	—	83.6	—	20

References

1. Y. K. Liu, S. Jiang, S. J. Li, L. Zhou, Z. H. Li, J. M. Li and M. F. Shao, *Appl. Catal. B*, 2019, **247**, 107-114.
2. Y. Pei, Y. C. Ge, H. Chu, W. Smith, P. Dong, P. M. Ajayan, M. X. Ye and J. F. Shen, *Appl. Catal. B*, 2019, **244**, 583-593.
3. G. Yan, X. T. Zhang and L. G. Xiao, *J. Mater. Sci.*, 2019, **54**, 7087-7095.
4. Z. Z. Ma, H. J. Meng, M. Wang, B. Tang, J. P. Li and X. G. Wang, *ChemElectroChem*, 2018, **5**, 335-342.
5. C. C. Liu, T. Gong, J. Zhang, X. R. Zheng, J. Mao, H. Liu, Y. Li and Q. Y. Hao, *Appl. Catal. B*, 2020, **262**, 118245.
6. X. F. Lu, L. F. Gu, J. W. Wang, J. X. Wu, P. Q. Liao and G. R. Li, *Adv. Mater.*, 2017, **29**, 1604437.
7. Y. Yan, B. Zhao, S. C. Yi and X. Wang, *J. Mater. Chem. A*, 2016, **4**, 13005-13010.
8. Y. J. Chen, C. Q. Dong, J. Zhang, C. Zhang and Z. H. Zhang, *J. Mater. Chem. A*, 2018, **6**, 8430-8440.
9. A. Wu, Y. Xie, H. Ma, C. Tian, Y. Gu, H. Yan, X. Zhang, G. Yang and H. Fu, *Nano Energy*, 2018, **44**, 353-363.
10. D. Das, S. Santra and K. K. Nanda, *ACS appl. mater. interfaces*, 2018, **10**, 35025-35038.
11. P. Y. Kuang, T. Tong, K. Fan and J. G. Yu, *ACS Catal*, 2017, **7**, 6179-6187.
12. Y. Wang, T. Williams, T. Gengenbach, B. Kong, D. Y. Zhao, H. T. Wang and C. Selomulya, *Nanoscale*, 2017, **9**, 17349-17356.
13. P. Ganesan, A. Sivanantham and S. Shanmugam, *J. Mater. Chem. A*, 2018, **6**, 1075-1085.
14. Y. Teng, X. D. Wang, J. F. Liao, W. G. Li, H. Y. Chen, Y. J. Dong and D. B. Kuang, *Adv. Funct. Mater.*, 2018, **28**, 1802463.
15. Z. L. Chen, R. B. Wu, Y. Liu, Y. Ha, Y. H. Guo, D. Sun, M. Liu and F. Fang, *Adv. Mater.*, 2018, **30**, 1802011.
16. J. G. Hou, B. Zhang, Z. W. Li, S. Y. Cao, Y. Q. Sun, Y. Z. Wu, Z. M. Gao and L. C. Sun, *ACS Catal*, 2018, **8**, 4612-4621.
17. X. Zhang, F. Zhou, W. Y. Pan, Y. Y. Liang and R. H. Wang, *Adv. Funct. Mater.*, 2018, **28**, 1804600.
18. Y. Wu, F. Li, W. L. Chen, Q. Xiang, Y. L. Ma, H. Zhu, P. Tao, C. Y. Song, W. Shang, T. Deng and J. B. Wu, *Adv. Mater.*, 2018, **30**, 1803151.
19. J. K. Gao, Y. H. Wu, M. T. Lu, Y. W. Li, P. P. He, S. B. Maddine and J. M. Yao, *Chem. Asian J.*, 2018, **13**, 3274-3280.
20. M. F. Fei, H. L. Shi, J. Zhao, N. Kang, W. Y. He, H. Li and F. C. Yang, *ChemCatChem*, 2018, **10**, 5174-5181.